USING TIME-INDEPENDENT ANALYSIS IN OPTIMIZING INVERTER EFFICIENCY FOR GRID-CONNECTED PHOTOVOLTAIC SYSTEMS

BY

OMAR ADEL EL BASSIOUNY

THESIS

Submitted in partial fulfillment of the requirements
for the degree of Master of Science in Electrical and Computer Engineering
in the Graduate College of the
University of Illinois at Urbana-Champaign, 2010

Urbana, Illinois

Adviser:

Associate Professor Patrick L. Chapman

ABSTRACT

A flexible and computationally efficient analysis technique for designing and evaluating grid-connected photovoltaic (PV) systems is introduced, which establishes a direct relationship between the inputs to the system, temperature and irradiance, and system performance criteria. For a given year, temperature and irradiance data are rearranged to form a statistical distribution, eliminating thereby the direct time-dependence. The proposed technique decomposes the PV system into three separate layers: an ambient conditions, a PV output, and a dc-ac conversion layer. It reveals important trends, otherwise obscured in the time-dependent view of the data.

The time-independent analysis technique is applied to the problem of optimizing inverter efficiency to improve the performance of residential PV systems. A parallel two-inverter configuration is proposed, where one inverter has a small rated power to handle the frequently occurring low-insolation conditions, while the other inverter is large enough to handle the high-insolation regime. The application of this new configuration leads to energy savings as well as efficiency and reliability improvements. A feasibility study taking into account the additional investments required to implement the suggested inverter configuration reveals that applying it under the current electricity prices does not make sense from the economic perspective. However, the two-inverter configuration can become an interesting option in the future as

energy prices continue to rise and more financial incentives for solar systems are introduced.

To my parents, for their love and support

ACKNOWLEDGMENTS

I would like to thank my adviser, Professor Patrick Chapman, for his guidance and support and for making my stimulating graduate studies in the power area at the University of Illinois possible. I am also grateful to my Everitt Lab friends, especially Sairaj Dhople, Jon Ehlmann, and Ali Davoudi for making the lab environment more pleasant and fun, and for providing moral, technical, and marketing support in addition to sharing valuable philosophical insights about life and the behavior of human beings. Last, but not least, I would like to thank all my friends, especially Ibtissam Ezzeddine and Samer Ghanem, for making my time in Champaign-Urbana more exciting, enjoyable, comfortable, homey, intellectually stimulating, fun, and for always believing in me.

TABLE OF CONTENTS

LIST OF TABLES

LIST OF FIGURES

CHAPTER 1

INTRODUCTION

Maximizing the energy yield of photovoltaic (PV) systems in order to generate the highest possible return on investment has been a persistent concern for customers and installers alike. In light of the current boom in solar markets sparked by government incentives and consumer awareness, improving the performance and reducing the cost of PV systems has become even more pressing. According to a recent report by the Interstate Renewable Energy Council, the residential sector continues to play a significant role in solar markets, reaching a remarkable 90% of all new grid-connected PV systems installed in 2008 [1]. Therefore, residential PV systems have been chosen to be the focus of this study.

This work proposes a new approach for analyzing the performance of PV systems in general. According to this approach, performance criteria that typically interest designers are plotted in 3-D graphs as a function of temperature and insolation – the actual system inputs – rather than the traditional depiction as a function of time. This new representation reveals important trends, otherwise obscured in the time-dependent view of the data. A layer structure is introduced, which increases simulation efficiency and flexibility. It decomposes the system into an ambient conditions layer, a PV output layer, and a dc-ac conversion layer.

When it comes to improving the performance of PV systems, many different solutions have been proposed. For example, in the case of inverters for photovoltaic applications, emerging architectures that challenge the traditional single-inverter paradigm in residential setups include string inverters, parallel inverters, and, more recently, dual inverters [2],[3]. However, most design practices and conventional system topologies fail to consider if suggested designs optimize system performance over the long term and are economically justified.

This work proposes an inverter configuration that is more efficient than conventional inverters for residential photovoltaic systems and provides insight into its economic feasibility. While the parallel configuration traditionally implies several identically sized inverters connected across the PV array [4], this study suggests a configuration involving two inverters of different sizes. Time-averaged conversion efficiency was improved by up to 22% using this configuration compared to a single, optimally sized inverter. The time-independent analysis technique mentioned above is used to simulate and validate these results.

Chapter 2 introduces the models used in the simulation of PV systems. Solar cells are modeled based on an equivalent circuit composed of a current source and a diode with series and parallel resistances. A number of cells are joined together to form PV modules whose electrical characteristics are defined by parameters from commercially available products. Inverters are modeled based on their conversion efficiency.

Chapter 3 presents the proposed alternative way of arranging temperature

and insolation data as a statistical distribution in 3-D. Temperature and solar irradiance data for different locations in the United States available through the National Renewable Energy Laboratory (NREL) were used. To illustrate the concept, case studies for residential PV systems in Colorado and Tennessee are conducted. The benefits of the proposed analysis technique are highlighted.

The proposed time-independent analysis technique is applied to the problem of optimizing inverter efficiency for residential applications. In Chapter 4, a new energy-efficient inverter configuration is introduced, where two inverters of different sizes are connected in parallel. Its performance is tested in the previously selected locations and compared to the currently dominant single-inverter topology.

In order to determine the economic feasibility of the proposed configuration, it is necessary to compare the value of the additional energy gained due to implementing this system to the extra capital invested in the additional hardware required. Chapter 5 includes a cost-benefit analysis over the entire system lifetime. Chapter 6 presents the main findings of this work.

CHAPTER 2

PHOTOVOLTAIC SYSTEM MODELING

In this chapter, we present the models that were used to simulate photovoltaic systems. Figure 2.1 shows the typical layout of such a system. The main hardware blocks are the PV array and the dc-ac converter, also known as the inverter. Both blocks are simulated in MATLAB®.

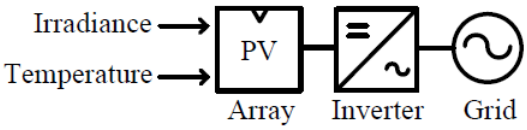

Figure 2.1: Residential grid-connected PV system layout.

2.1 Modeling photovoltaic cells and arrays

Photovoltaic arrays are typically formed by arranging individual modules in series to form strings, which are then connected in parallel. Modules are in turn composed of PV cells. There are several ways to model PV cells and modules, such as the power-temperature coefficient model, the PVFORM model, and the bilinear interpolation model [5]. The power-temperature coefficient model applies a temperature correction to the maximum power value provided in manufacturer's data sheets to account for departures in cell temperature from those at standard test conditions (STC). The power-temperature coefficient model has the advantage of being simple. However,

its accuracy is limited to modeling single-crystal silicon and amorphus silicon (a-Si) PV modules. The bilinear interpolation model, which implements a method in which four I-V curves could be used to bilinearly interpolate an I-V curve with respect to both irradiance and PV cell temperature, was found to be the most effective at reducing the error statistics for modeling the maximum power output of different types of modules [5].

This study uses a model that achieves a compromise between the simplicity of the power-temperature coefficient model and the accuracy of the bilinear interpolation model. Solar cells are modeled based on the equivalent circuit shown in Fig. 2.2, which is composed of a current source and a diode with series and parallel resistances.

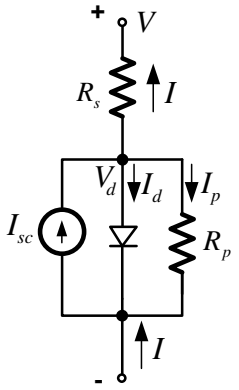

Figure 2.2: Equivalent circuit of the PV cell model used.

Equation 2.1 establishes the relationship between the cell voltage, V, and cell current, I [6].

$$\begin{aligned} I &= I_{sc} - I_d - I_p \\ &= I_{sc} - I_0(e^{qV_d/nkT_c} - 1) - \frac{V_d}{R_p} \\ &= I_{sc} - I_0\left\{e^{\left[\frac{q(V+IR_s)}{nkT_c}\right]} - 1\right\} - \left(\frac{V+IR_s}{R_p}\right) \end{aligned} \tag{2.1}$$

Here, I_{sc} is the short circuit current, I_d is the diode current, I_p is the current on the parallel resistor, I_0 is the saturation current, V_d is the diode voltage, n is the diode ideality factor, k represents Boltzmann's constant, T_c is the cell temperature, R_s is the series resistance, and R_p is the parallel resistance. The dependence of the cell temperature on the ambient temperature and solar irradiance is characterized by the following relationship [6]:

$$T_c = T_a + \left[\frac{(NOCT - 20°C)}{0.8}\right] S \tag{2.2}$$

where T_a is the ambient temperature in °C, $NOCT$ is the nominal operating cell temperature, and S is the insolation level in suns (1 kW/m^2). The diode ideality factor is a function of the cell temperature as follows [6]:

$$n = \frac{11600}{T_c + 273.15°C} \tag{2.3}$$

The deviation of the open circuit voltage, V_{oc}, and the short circuit current from their values at STC due to variations in ambient conditions are characterized by

$$V_{oc}(T_c, S) = V_{oc,STC} - \alpha_{V_{oc}}(T_c - 25) \tag{2.4}$$

and

$$I_{sc}(T_c, S) = [I_{sc,STC} - \alpha_{I_{sc}}(T_c - 25)]S \tag{2.5}$$

where $V_{oc,STC}$ and $I_{sc,STC}$ are the open circuit voltage and short circuit current at STC, respectively, and $\alpha_{V_{oc}}$ and $\alpha_{I_{sc}}$ are the temperature coefficient of V_{oc} and I_{sc}, respectively. The saturation current can be found based on

the fact that the cell current is zero when the cell voltage is equal to the open circuit voltage. In this case it can be calculated using the following formula:

$$I_0 = \left[\frac{I_{sc}(T_c, S) - \frac{V_{oc}(T_c,S)}{R_p}}{e^{nV_{oc}} - 1} \right] \tag{2.6}$$

Since equation (2.1) is nonlinear, an iterative procedure is used to find the I-V and P-V curves for solar cells under various ambient conditions. Solar cells can be put together in series and in parallel to yield the total module output. The module P-V curve can then be used to find the maximum power output for the specified combination of temperature and insolation.

All the parameters used in these equations can be found in the module manufacturer's specification sheets. A number of parameters can be used to simulate various modules. In this study, the Kyocera KD210GX-LPU module was used as a sample [7]. Other commercially available modules can be used equivalently. Key electrical performance parameters that are inputs to this model are given in Table 2.1, along with their corresponding values for this particular module type.

Table 2.1: Key electrical performance parameters of the Kyocera KD210GX-LPU module under STC.

Parameter	**Value**
Maximum power (P_{max})	210 W
Open circuit voltage (V_{oc})	33.2 V
Short circuit current (I_{sc})	8.58 A
Temperature coefficient of V_{oc}	-0.12 V/°C
Temperature coefficient of I_{sc}	5.15×10^{-3} A/°C
Number of cells	54 (9×6)
NOTC	49 °C

The I-V and P-V curves of this Kyocera module under STC are given in Fig. 2.3 (a) and (b), respectively. The maximum power, short circuit current, and open circuit voltage values are in agreement with those specified by the manufacturer in Table 2.1, which validates the model.

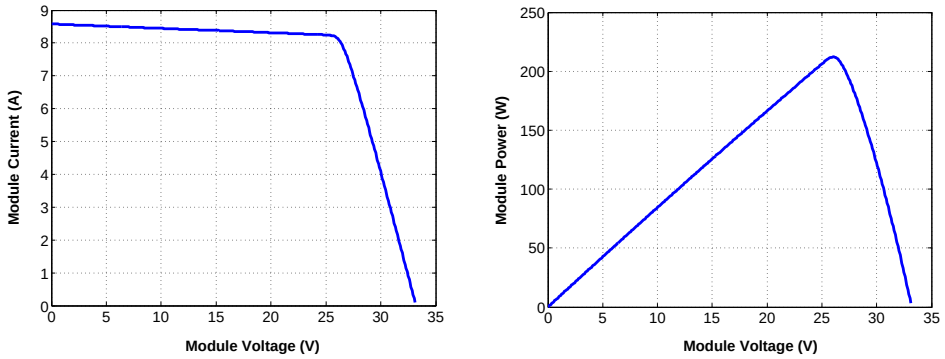

(a) I-V curve (b) P-V curve

Figure 2.3: I-V curve (a) and P-V curve (b) of the simulated Kyocera module under STC.

The series and parallel resistance values are not indicated by the manufacturer. They have been adjusted in the model to achieve the specified performance under STC. In this case, these values were chosen to be 0.5 Ω and 50 Ω for the series and parallel resistance, respectively.

2.2 Modeling inverters

It is common practice to model inverters by their conversion efficiency profile. There have been consistent efforts to develop analytical expressions to relate the output ac power of inverters to the input dc power. Examples for these expressions are the quadratic equation [8], the double quadratic equation [9], and the Sandia model [10]. Most of these models have to balance the trade-off between accuracy and complexity. Alternatively, this study takes advantage of overall efficiency versus fractional loading data provided by

Photon Magazine at various maximum power point (MPP) voltages [11]. The data is based on experimental tests that are conducted on a regular basis for a large number of commercially available inverters. The efficiency profile of the SB SMA 2100TL inverter, which was used as a sample in this analysis, is shown in Fig. 2.4. It has a dc nominal power of 2,020 W and a maximum efficiency of 96%.

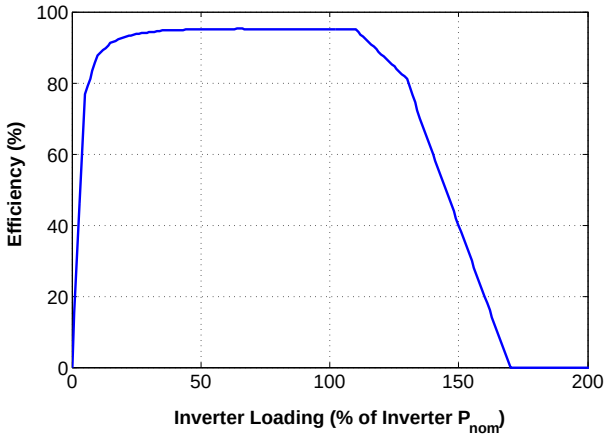

Figure 2.4: Efficiency profile of the SB SMA 2100TL inverter.

CHAPTER 3

TIME-INDEPENDENT ANALYSIS

3.1 Limitations of time-dependent analysis

Photovoltaic system performance criteria, such as energy yield and overall system efficiency, are typically evaluated in a given location over a year to capture the effects of seasonal variations in ambient conditions. The result is typically a two-dimensional graph of some performance criterion as a function of time. For example, Fig. 3.1 shows the maximum power point tracker (MPPT) and inverter output of a 2 kW system in Colorado during four days in July 2008.

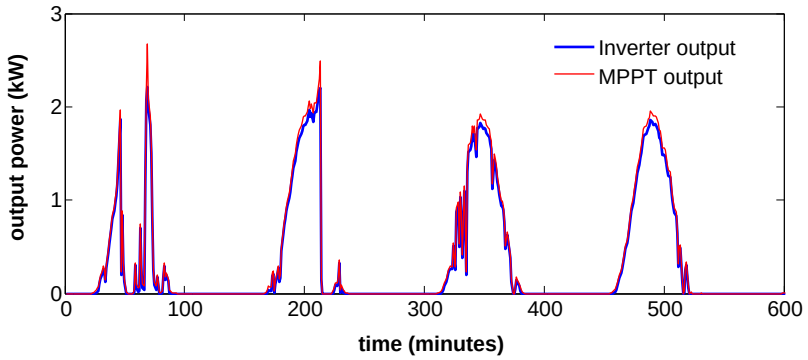

Figure 3.1: 2 kW System in Colorado: output power over a period of four days (July 2008).

In order to create these types of graphs, solar irradiance and temperature data are collected at small-enough time intervals to capture system dynamics accurately. Studies have revealed that hourly averages hide important irradiation peaks that need to be considered for the purpose of accurate sim-

ulation [12]. One- or five-minute intervals have been found to be more appropriate. However, since this involves thousands of data samples, calculating performance criteria for balance-of-system components, such as inverters, as a function of time introduces a significant computational burden. Modifying parameters in the system entails repeating time-consuming calculations, which reduces simulation flexibility. In addition, observing the performance as a function of time does not reveal much more than cyclical seasonal variations, as in Fig. 3.1. These issues highlight the need for a more flexible and computationally efficient method for designing and evaluating grid-tied residential PV systems.

3.2 Introduction to time-independent analysis

The suggested time-independent analysis technique establishes a direct relationship between the inputs to the system, temperature and irradiance, and system performance criteria. For a given year, temperature and irradiance data are rearranged to form a statistical distribution, eliminating thereby the direct time-dependence. The output power of a PV system can be evaluated based on a combination of input temperature and irradiance. Therefore, if a certain combination reoccurs, there is no need to repeat the same calculation. This concept allows for the efficient reuse of the temperature-irradiance data in various calculations, which considerably saves simulation time. In addition, the suggested technique reveals important trends, otherwise obscured in the time-dependent view of the data.

3.3 Layer structure

The suggested approach decomposes the PV system into three separate layers as demonstrated in Fig. 3.2: ambient conditions, PV, and dc-ac conversion layers. These layers are stacked on top of each other to yield the output of

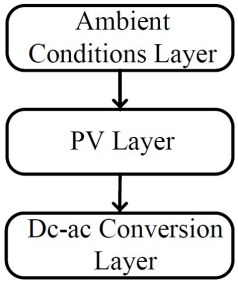

Figure 3.2: Layer-view of the PV system

the simulated system. For example, overlaying the PV layer on the ambient conditions layer provides the output of the PV array. Adding the dc-ac conversion layer yields the overall system output. This structure introduces enhanced flexibility, since each layer can be modified independently. Consequently, only parts of a simulation have to be repeated instead of the entire simulation every time a parameter is changed. The layered structure is a flexible and efficient tool for designers, because different system configurations can be seamlessly tested and system components can be independently optimized for performance.

3.3.1 Ambient conditions layer

The ambient conditions layer captures the maximum ranges of temperature and irradiance and divides these into intervals to form temperature and irradiance (T-I) sectors. An ambient conditions probability distribution is formulated by weighting each sector by its frequency of occurrence. In this

study, minutely daytime solar irradiance and ambient temperature data from the National Renewable Energy Laboratory (NREL) are used [13]. The temperature and irradiance intervals have been set to be 2 °C and 50 W/m^2, respectively. The mean sector temperature (MST) and mean sector irradiance (MSI) are defined as the midpoint of each temperature and irradiance interval, respectively. Two locations in the U.S. with different ambient conditions were chosen to illustrate this idea. The ambient conditions layers for the year 2008 are shown in Fig. 3.3 (a) and (b) for Tennessee and Colorado, respectively.

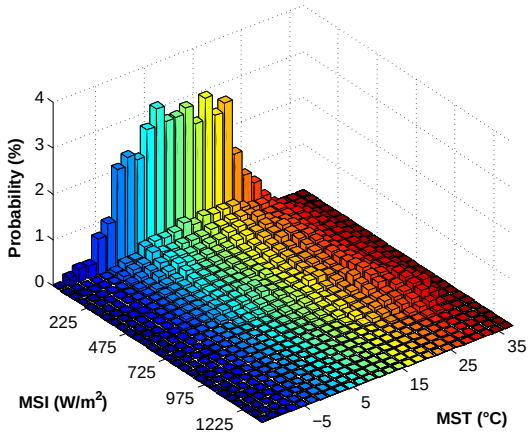

(a) Tennessee

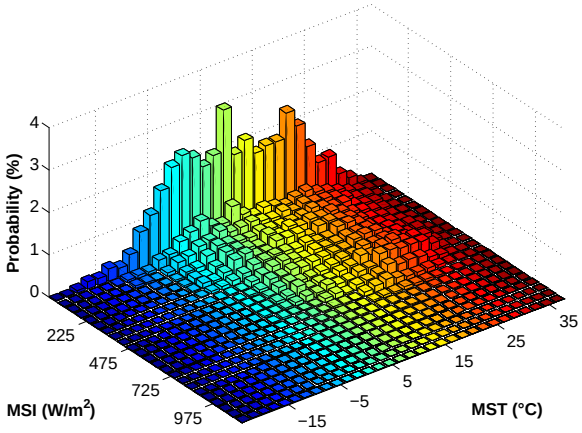

(b) Colorado

Figure 3.3: Ambient conditions layers representing the year 2008 in (a) Tennessee and (b) Colorado.

Differences between the temperature-irradiance distributions in both locations can be clearly seen from the figures. This layer enables us to determine which T-I sectors occur more often than others. For example, it can be seen that low insolation conditions prevail during most of the day in both locations. This information can be then used to optimize system design.

3.3.2 PV layer

The PV layer is created by evaluating the maximum power output of the PV array at each T-I combination. This can be done using the photovoltaic cell model developed in Chapter 2. Figure 3.4 presents the PV layer based on the selected Kyocera module over a range of temperature and irradiance. This layer is independent of time and location. It can be separately adjusted and plugged into a simulation without affecting other layers.

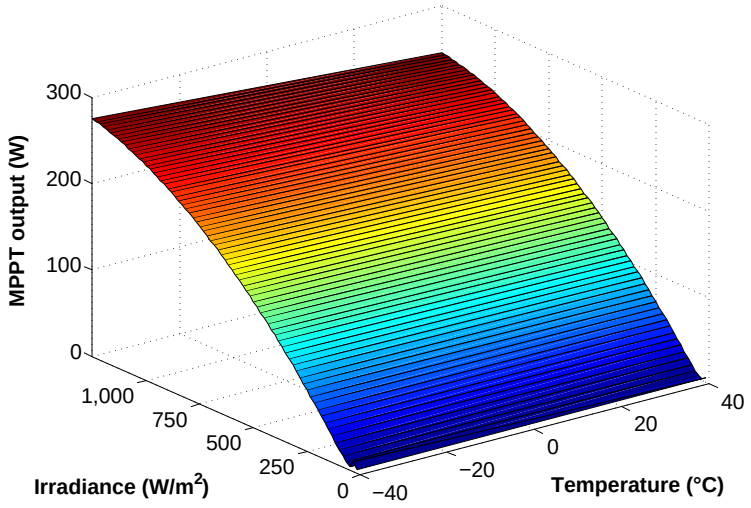

Figure 3.4: PV layer based on the selected Kyocera module.

3.3.3 Dc-ac conversion layer

As mentioned earlier in Chapter 2, inverters are modeled by their conversion losses. Figure 3.5 demonstrates the dc-ac conversion layer representing the efficiency profile of the SMA 2100TL inverter depicted in this study.

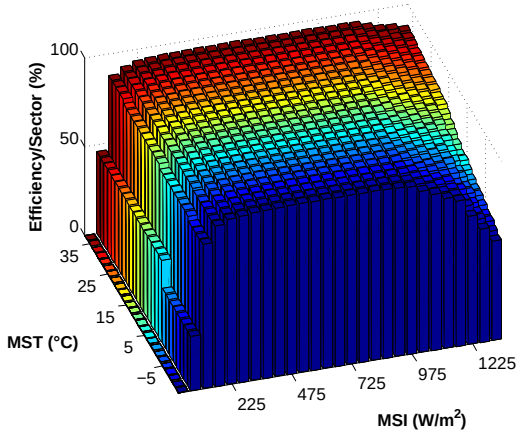

Figure 3.5: Dc-ac conversion layer representing the SMA 2100TL inverter.

This layer is obtained by matching each output power level associated with a particular T-I sector with the conversion efficiency corresponding to the resulting loading level as specified by the efficiency profile in Fig. 2.4. Since the efficiency profile of an inverter carries all necessary information to create the dc-ac conversion layer, it is relatively easy to simulate different inverters. Note the decrease in efficiency in the low and very high insolation sectors. Also, it appears that efficiency decreases with temperature.

The layered structure is a useful tool for designers, as different system configurations can be seamlessly tested and balance-of-system components can be optimized for performance. In addition, the layered structure enhances simulation flexibility by allowing the parameters of each layer to be modified independently. Therefore, calculations need only be repeated for that layer instead of for the entire system. In addition, the suggested technique

reveals important trends, otherwise obscured in the time-dependent view of the data, which does not reveal much more than cyclical seasonal variations.

CHAPTER 4

USING TIME-INDEPENDENT ANALYSIS IN INVERTER OPTIMIZATION

To demonstrate the applicability of the proposed technique, it is applied to the problem of optimizing inverter efficiency in order to improve the performance of residential solar systems. As mentioned previously, various architectures that challenge the traditional single-inverter paradigm in residential PV installations have been proposed. Examples are string inverters, parallel inverters, and, more recently, dual inverters [1],[2]. However, most design practices and conventional system topologies fail to consider if suggested designs optimize system performance over the long term and are economically justified. The latter will be discussed in Chapter 5 with regard to the suggested configuration.

4.1 Proposed inverter configuration

This work proposes a new parallel inverter architecture based on two generic observations. First, in many locations in the U.S. (and indeed the world over), the average period of time when full-sun is received is minimal. For instance, Fig. 3.3 shows that low-insolation conditions are fairly dominant. Second, the efficiency of most commercially available inverters drops significantly with dc input power [14], which in turn significantly drops with insolation. This fact is demonstrated by the dc-ac layer in Fig. 3.5. These observations suggest that inverters sized according to the dc rating of the PV

array may not operate efficiently over the course of the year.

While the parallel configuration has traditionally implied several identically sized inverters connected across the PV array [3], this work proposes a parallel-inverter configuration built with inverters rated at different power levels to address the drop in system efficiency during low-insolation conditions. The suggested topology is shown in Fig. 4.1.

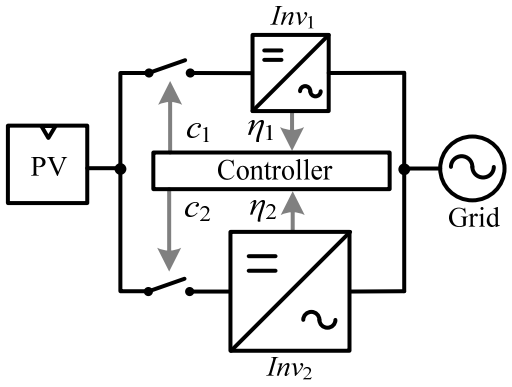

Figure 4.1: Suggested system configuration.

The first inverter, Inv_1, has a smaller rated power to handle the frequently occurring low-insolation conditions, while the larger inverter, Inv_2, handles the high-irradiance, high-power regime. A simple control strategy optimizes system efficiency by ensuring that both inverters do not stray into low-efficiency operating regimes. Based on the minutely efficiency information from the two inverters (η_1, η_2), control signals (c_1, c_2) dictate which inverter should be tied to the grid, such that only one of the two inverters is operating at each point in time. Note that in this study, it is assumed that the efficiency profile remains the same for inverters of different sizes.

4.2 Performance of suggested topology

Figures 4.2 (a) and (b) show the energy yield of PV systems in Tennessee and Colorado, respectively, during 2008. Both 9.2 kW systems are applying the suggested inverter configuration. The figure displays the amount of kilowatt hours contributed by each T-I sector per year, which is obtained by combining the ambient conditions, PV, and dc-ac conversion layers.

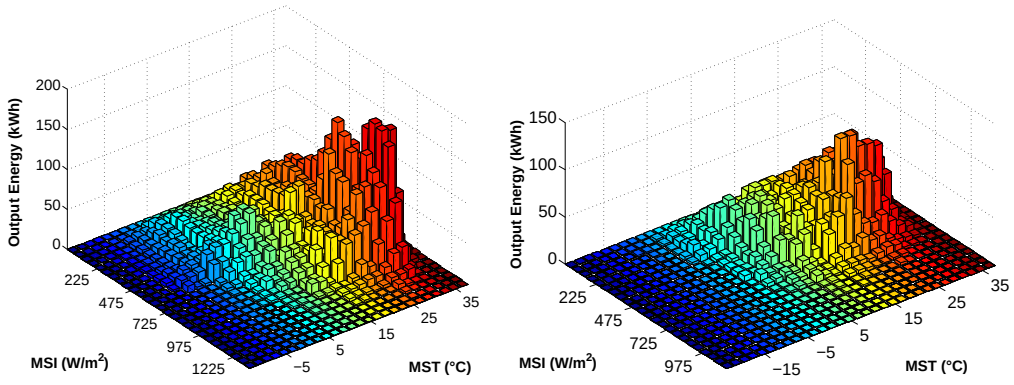

(a) Tennessee (b) Colorado

Figure 4.2: Energy yield during 2008 of PV systems applying the proposed inverter configurations in (a) Tennessee and (b) Colorado.

Figure 4.3 shows conversion losses as a function of the two inverters' rated power in Tennessee, which can be used to find the optimal two-inverter combination. In this case, losses are minimized by the combination of a 2.3 kW and a 9.1 kW inverter.

Tables 4.1 and 4.2 present key findings of this study, including a comparison with the single-inverter configuration. In Tennessee, savings of 120 kWh per year (0.83%) can be achieved with the proposed system compared to a system using a single, optimal inverter.

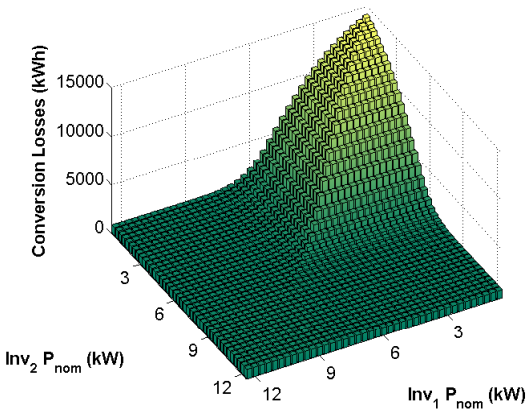

Figure 4.3: Conversion losses as a function of the rated power of the two inverters for a 9 kW system in Tennessee.

In Colorado, the situation is similar with savings of 86 kWh per year (1.07%). Furthermore, the system implementing the optimal two-inverter combination experiences an average efficiency increase of 9.7% and 22.3% in Tennessee and Colorado, respectively, compared to the traditional system. This suggests that the proposed configuration would be more beneficial in low-irradiance, low-temperature locations.

Table 4.1: PV system performance in Tennessee using the parallel two-inverter vs. the single-inverter configuration.

	Single Inverter	**Two Inverters**	
Optimal inverter(s) P_{nom} (W)	8,670	2,340	9,130
Loading (% of time)	100	63.9	36.1
Average inverter efficiency (%)	54.8	64.5	
Overall system efficiency (%)	11.02	11.57	
Losses (kWh/year)	898	778	
Losses (% of total energy yield)	6.18	5.35	
Net energy yield (kWh/year)	13,632	13,752	

Table 4.2: PV system performance in Colorado using the parallel two-inverter vs. the single-inverter configuration.

	Single Inverter	**Two Inverters**	
Optimal inverter(s) P_{nom} (W)	6,470	760	7,180
Loading (% of time)	100	52.9	47.1
Average inverter efficiency (%)	56.84	79.15	
Overall system efficiency (%)	10.92	11.75	
Losses (kWh/year)	522	436	
Losses (% of total energy yield)	6.5	5.43	
Net energy yield (kWh/year)	7,511	7,598	

The proposed inverter structure also increases system reliability due to the inherent structural redundancy. Each of the two inverters ends up operating about 50% of the time instead of 100% in the single-inverter case. This increases the lifetime of the inverters and potentially eliminates the need for costly replacements over the lifetime of the system.

CHAPTER 5

FEASIBILITY STUDY

In the previous chapter, it was established that the two-inverter configuration improves efficiency and increases energy harvest compared to the traditional single-inverter topology. The next logical step is to study its economic feasibility. The outcome of such a study might not be very obvious. On the one hand, installing two inverters instead of one implies – in most cases – increased initial costs. On the other hand, energy-yield-based optimization might result in favorable payback of the extra capital invested in a second inverter, especially in energy markets with different forms of economic incentives for solar systems.

The following analysis compares the lifetime costs and the value of the energy produced by a traditional system (system A) with a system using the suggested inverter topology (system B). The economic feasibility of the suggested topology is established if the analysis shows that the income generated by system B, namely the difference between the value of the energy produced and the system costs, is higher than the income generated by system A over the lifetime of each system. Again, both locations, Tennessee and Colorado, are considered.

5.1 System revenues

The energy yield of a solar system can significantly vary depending on the season. For example, Fig. 5.1 shows that in Tennessee, about 1,800 kWh are produced in June compared to only 600 kWh in February of the same year.

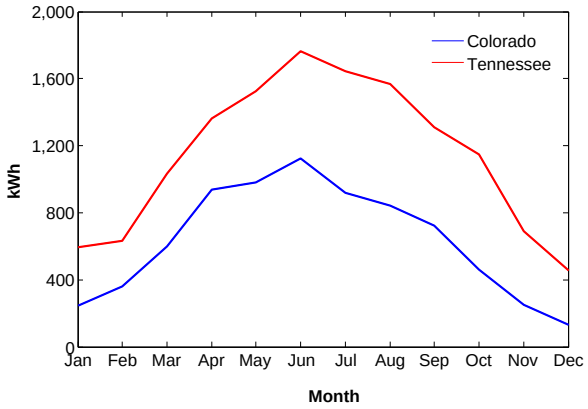

Figure 5.1: Monthly energy harvest of system B in Tennessee and Colorado in 2008.

At the same time, electricity prices also fluctuate depending on supply and demand. Therefore, in order to accurately assess the economic value of the energy produced by a solar system, it is necessary to compare the monthly energy yield to the monthly electricity price trends. Figure 5.2 demonstrates the monthly variation of average electricity prices in 2009 according to the Energy Information Administration (EIA) [15].

By examining Fig. 5.1 and 5.2, it is clear that the electricity price trends are not very different from the solar system's energy production trends. This is a favorable situation, since it implies that a large fraction of the energy produced in a year (more than 56%) is valued at peak prices. This fact also justifies the importance of considering monthly energy production and monthly price variation in our analysis.

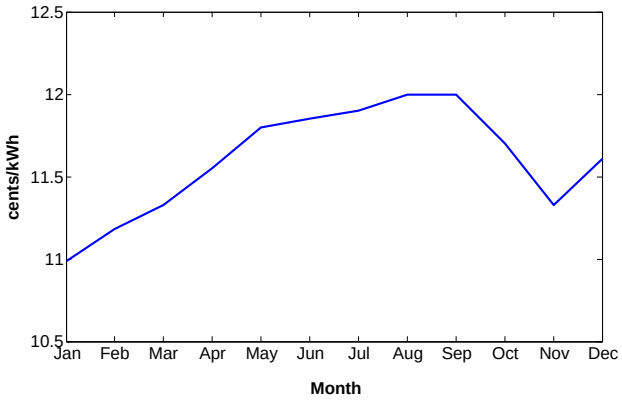

Figure 5.2: Electricity prices by month in 2009 according to the Energy Information Administration.

There is a wide spectrum of financial incentives offered by utilities, states, the federal government, and even non-profit organizations. They range from production-based incentives such as feed-in tariffs to investment-based incentives such as tax credits, rebate programs, loans, and grants [16]. The variety, number, and significance of financial incentives for solar systems depend on the offers made by different institutions operating in a certain location.

For the purposes of this study, however, the deciding factor is the price at which the electricity produced by the solar system, also called solar electricity, is sold. That is the case because the analysis conducted here compares the economic feasibility of two identically sized solar systems A and B, which are operating at the same location. Therefore, both systems enjoy the same financial incentives offered to solar system installers. Solar electricity prices might include feed-in tariffs and other incentives, which contribute to the final pricing of the energy produced by the system. Hence, the only difference between systems A and B – in terms of their economics – is the amount of energy produced by each system and the economic value of this energy.

Tables 5.1 and 5.2 compare the value of the energy produced by systems A and B over their lifetime in Colorado and Tennessee, respectively. The energy value of a system over its lifetime is calculated by multiplying the amount of monthly energy produced by the monthly price of electricity given by the EIA, evaluated over the estimated system life.

Table 5.1: Comparison of system A and B energy production and energy value in Colorado.

Performance	**System A**	**System B**
DC system rating (W)	9,200	9,200
Estimated system life (years)	25	25
Energy performance (kWh/year)	7,511	7,598
Energy production over lifetime of system (kWh)	187,775	189,950
Revenue of the system over its lifetime ($)	**21,995.00**	**22,202.00**

Table 5.2: Comparison of system A and B energy production and energy value in Tennessee.

Performance	**System A**	**System B**
DC system rating (W)	9,200	9,200
Estimated system life (years)	25	25
Energy performance (kWh/year)	13,632	13,752
Energy production over lifetime of system (kWh)	340,800	343,800
Revenue of the system over its lifetime ($)	**39,797.00**	**40,141.00**

Note that the electricity price used here is the regular price of electricity in the residential sector and not the price of solar electricity. The latter will be considered at later stages of the analysis. The results shown in Tables 5.1 and 5.2 highlight the tremendous impact of location and ambient condition on energy production and income generation of a solar system. The energy value of both systems A and B over their lifetime in Tennessee is almost dou-

ble that in Colorado. Comparing the performance of systems A and B, we find that the revenue of system B over its lifetime is higher than the revenue of system A by about $207 under the EIA prices in Colorado. In Tennessee, we have a similar situation, where the revenue incurred by system B is higher than system A by $344.

5.2 System costs

After studying the revenues of systems A and B, the next step is to evaluate the cost of both systems. The cost of a solar system can be broken up as demonstrated in Tables 5.3 and 5.4 for Colorado and Tennessee, respectively. Note that the module cost is the same for system A and system B. The costs of installation and balance of system components have been increased for system B to account for the extra hardware (control system and connections) and the extra labor required to set up the system.

Table 5.3: Cost breakdown and total cost of systems A and B in Colorado.

Item	**System A**	**System B**	
Module cost ($/W)	4	4	
Inverter cost ($/W)	0.61 (6470 W)	0.88 (760 W)	0.60 (7180 W)
Balance of system cost ($/W)	1	1.005	
Installation ($/W)	2	2.005	
Subtotal ($)	68,340.23	69,438.46	
Tax rate (%)	7.50	7.50	
Up-front system cost ($)	**73,465.75**	**74,646.34**	

Table 5.4: Cost breakdown and total cost of systems A and B in Tennessee.

Item	**System A**	**System B**	
Module cost ($/W)	4	4	
Inverter cost ($/W)	0.57 (8670 W)	0.74 (2340 W)	0.57 (9130 W)
Balance of system cost ($/W)	1	1.005	
Installation ($/W)	2	2.005	
Subtotal ($)	69,357.51	71,380.11	
Tax rate (%)	7.50	7.50	
Up-front system cost ($)	**74,559.32**	**76,733.62**	

The inverter cost has been calculated for the optimal inverters required for both systems A and B based on Equation 5.1, which calculates the cost per watt, *P(x)*, as a function of inverter nominal power, x.

$$P(x) = -0.1269 \times log(x) + 1.7225 \tag{5.1}$$

This equation was obtained by fitting more than 150 data points of recent prices of inverters of different sizes currently available on the market. Plotting the cost-per-watt versus inverter size yields the curve shown in Fig. 5.3.

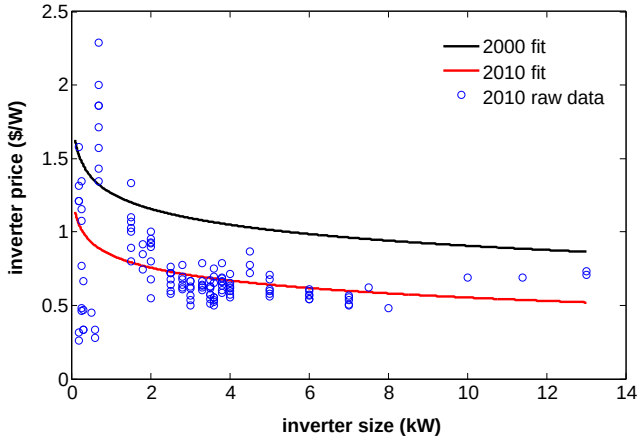

Figure 5.3: Cost-per-watt versus inverter size using inverter price data from 2000 and 2010.

Figure 5.3 also contrasts this fit to a similar one obtained using data from the year 2000 and published in 2002 [4]. It is interesting to see that the cost of inverters as a function of size has decreased almost with a constant downward shift of about \$0.38/W. The shape remained largely preserved with smaller inverters being more expensive per watt than larger inverters. The curve is a convenient way to estimate the cost of an inverter of a specified size.

As expected, the total up-front costs of system B are higher than system A. System B is \$2,174.30 more expensive in Tennessee and \$1,180.60 more expensive in Colorado, mostly due to the higher cost of the two-inverter combination.

5.3 Net income and future prices

Tables 5.5 and 5.6 summarize the results from the previous two sections. First of all, the values in the two tables show that both systems A and B are not economically feasible under regular electricity prices neither in Tennessee nor in Colorado, even though the losses in Tennessee are smaller. This justifies the current need for financial incentives for solar energy systems.

Table 5.5: Summary of economic analysis based on 2009 Energy Information Administration electricity prices (Colorado).

	System A	**System B**	**Difference**
Total revenues (\$)	21,995.00	22,202.00	207.00
Total costs (\$)	73,465.75	74,646.34	1,180.60
Net income (\$)	– 51,470.75	– 52,444.34	– 973.60

Furthermore, one can see that the higher up-front costs associated with sys-

tem B exceed the additional revenues gained due to higher efficiency, again as evaluated under regular residential electricity prices. The difference between the losses of both systems B and A amounts to $1,830.30 in Tennessee and $973.60 in Colorado, which favors system A.

Table 5.6: Summary of economic analysis based on 2009 Energy Information Administration electricity prices (Tennessee).

	System A	**System B**	**Difference**
Total revenues ($)	39,797.00	40,141.00	344.00
Total costs ($)	74,559.32	76,733.62	2,174.30
Net income ($)	– 34,762.32	– 36,592.62	– 1,830.30

As mentioned earlier, the electricity price is the main factor that affects the economic feasibility of B compared to system A. Let us now consider the effect of using solar electricity prices instead of regular electricity prices in our analysis, in a scenario where production financial incentives are present. In addition, this scenario includes future increases in regular electricity prices. The goal is to determine if there is a price at which system B becomes more profitable than system A. Figure 5.4 does just that. It shows the difference between the net income (NI) of systems A and B in Colorado and Tennessee as a function of average solar electricity price.

Figure 5.4 indicates that system B becomes more profitable than system A at a solar electricity price of about $0.54 per kWh in Colorado and $0.72 per kWh in Tennessee. This fact highlights two issues. First, system B is in general more profitable than system A in Colorado. This confirms the previous finding that the proposed two-inverter configuration is more beneficial in areas with low-insolation, although this advantage becomes less significant as

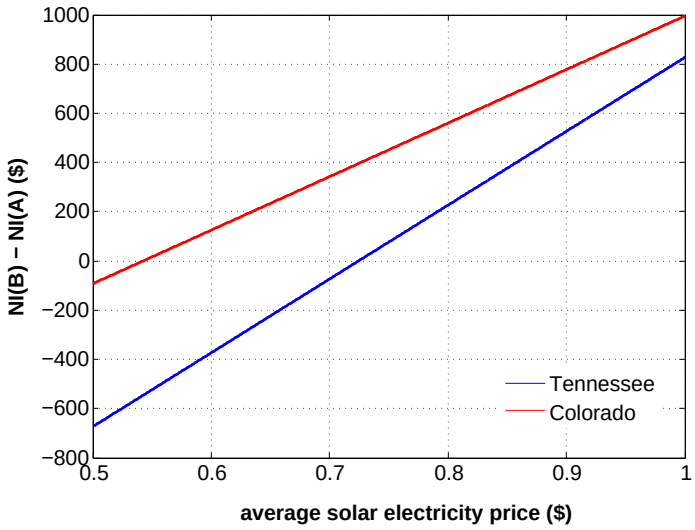

Figure 5.4: The difference between the net income (NI) of system B and the NI of system A as a function of average solar electricity price in Colorado and Tennessee.

the price of electricity increases. Second, the solar electricity price at which the suggested configuration becomes more profitable than the traditional system is not too far from current solar electricity prices. According to *Solarbuzz*, the average solar electricity price in 2009 is about $0.36 per kWh [17].

In summary, one can say that while the proposed configuration is not economically feasible at this point in time, it will start becoming more advantageous than the traditional system in most locations once solar electricity prices exceed $0.8 per kWh. At a solar electricity price of $1.00 per kWh, the proposed configuration generates an extra $1,000 in Colorado and more than $800 in Tennessee compared to a traditional system.

Figure 5.5 shows the percent change in net income due to the application of the proposed configuration. At a solar electricity price of $1 per kWh, the net income generated increases by about 0.9% and 0.35% in Colorado and

Tennessee, respectively, by using the proposed configuration as opposed to the traditional system.

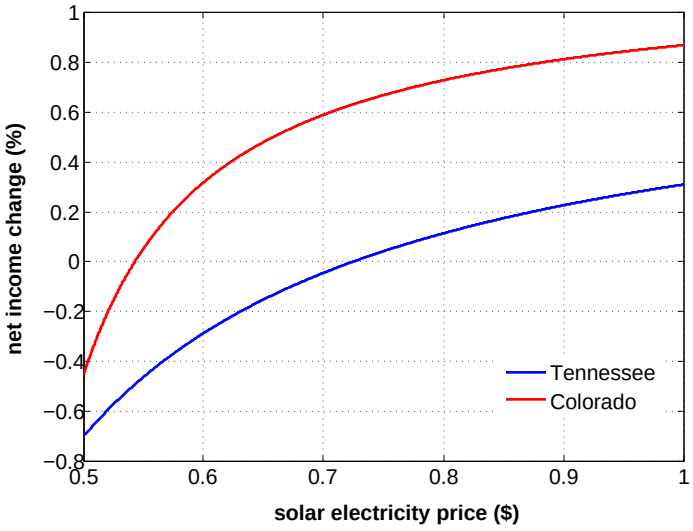

Figure 5.5: Percent change in net income due to applying the suggested inverter configuration in Tennessee and Colorado.

It is important to note here that while this study takes into account future increases in electricity prices and their impact on the economic feasibility of the suggested configuration, it does not incorporate the fact that inverter prices are expected to drop in the future. This is clearly displayed in Fig. 5.3, which compares inverter prices in the years 2000 and 2010, and shows a decrease of about \$0.38/W in inverter prices over the course of those ten years.

As mentioned earlier, the higher inverter costs associated with the suggested system configuration constitute by far the largest fraction – over 90% – of the cost difference between the the suggested configuration and the traditional system. As the inverter industry matures, inverter prices will keep decreasing, making the cost of the suggested configuration close to that of the traditional system with a single inverter. In this case, the higher revenues

generated by the two-inverter combination due to the improved energy yield and increased electricity prices will make the suggested system configuration even more profitable.

CHAPTER 6

CONCLUSION

A new time-independent approach for evaluating and monitoring photovoltaic systems that is based on establishing a direct relationship between the inputs to the system, temperature and insolation, and various performance criteria is proposed. Compared to the traditional method of studying the performance of PV systems as a function of time, the suggested layered, statistical approach is more efficient and provides more flexibility in simulation, testing, and design. In addition, it reveals important trends otherwise obscured in the time-dependent view of data.

The application of this technique to two 9.2 kW systems in Tennessee and Colorado clearly showed that low insolation conditions occur more than 50% of the time over the course of a year. At the same time, most inverters suffer from poor efficiency under low loading conditions. These observations led to the idea of implementing an optimized two-inverter configuration connected in parallel across the entire system. One inverter is small to operate in the high-efficiency regime under low insolation, and the other one is large to optimally address high-insolation conditions.

The performance of a system using the suggested inverter configuration is compared to the performance of a traditional system with a single inverter. The study revealed that there are benefits associated with the proposed two-

inverter combination when it comes to reliability, because each of the two inverters ends up operating about 50% of the time instead of 100% in the single-inverter case, which increases the lifetime of the inverters. More importantly, however, energy savings of 0.83% and 1.07% can be achieved in Tennessee and Colorado, respectively. Furthermore, the average efficiency of the inverting unit increased by 9.7% and 22.3% in Tennessee and Colorado, respectively, which suggests that the proposed configuration is more beneficial under low-irradiance, low-temperature conditions.

After clearly demonstrating the benefits of the new inverter topology in terms of enhanced reliability, prolonged lifetime, energy savings, and improved efficiency, the remaining aspect was to study whether the implementation of this topology is economically feasible, meaning that the investment in the additional capital required to install this kind of system is justified. The feasibility analysis revealed that a solar system in Tennessee and Colorado will only start being profitable at a solar electricity price of roughly \$0.22 and \$0.38 per kWh, respectively. Furthermore the economic analysis showed that a system implementing the proposed inverter configuration will not become more profitable than the traditional system until the price of solar electricity reaches about \$0.54 per kWh in Colorado and \$0.72 per kWh in Tennessee. Again, this confirms the previous finding that the proposed two-inverter configuration is more beneficial in areas with low insolation.

While the proposed configuration is not economically feasible at this point in time, it will start becoming more advantageous than the traditional system in most locations once solar electricity prices exceed \$0.8 per kWh. At a solar electricity price of \$1.00 per kWh, the proposed configuration generates

an extra $1,000 in Colorado and more than $800 in Tennessee compared to a traditional system, which corresponds to a net income increase of about 0.9% and 0.35%, respectively. Since energy prices steadily continue to rise, this might not be a very far-fetched scenario, especially in markets that offer different forms of financial incentives for renewable energy systems. In addition, reductions on the cost side can be possible as inverter prices continue to decline with time. The proposed configuration could also eliminate the need for costly inverter replacements during the lifetime of the PV system, making it more economically favorable over the traditional single-inverter topology.

These findings suggest that the extra benefits of improving the efficiency of central inverters using the proposed two-inverter approach do not necessarily lead to the desired high return on investment, even in the presence of high electricity prices in the future. A more lucrative alternative might be investigating the use of distributed inverters in order to increase module-level instead of inverter-level energy harvest.

REFERENCES

[1] L. Sherwood. (2010, Jul.). U.S. Solar Market Trends 2008. Interstate Renewable Energy Council. [Online]. Available: http://irecusa.org/irec-programs/publications-reports/.

[2] C. Meza, J.J. Negroni, F. Guinjoan, and B. Domingo, "Inverter comparative for residential PV grid connected system," in *Proc. IECON*, 2006, pp. 4361-4366.

[3] C. Attaianese, M. Di Monaco, V. Nardi, and G. Tomasso, "Dual inverter for high efficiency PV systems," in *Proc. IEEE International Electric Machines and Drives Conference*, 2009, pp. 818-825.

[4] A. Pregelj, M. Begovic, and A. Rohatgi, "Impact of inverter configuration on PV system reliability and energy production," in *Proc. IEEE Photovoltaic Specialists Conference*, May 2002, pp. 1388-1391.

[5] B. Marion, "Comparison of predictive models for photovoltaic module performance," in *Proc. 33rd IEEE Photovoltaic Specialists Conference*, May 2008, pp. 1-6.

[6] G. M. Masters, *Renewable and Efficient Electric Power Systems*. Hoboken, NJ: Wiley-Inter Science, 2004.

[7] KYOCERA-KD210GX-LP module specification sheet. The Americas: Kyocera Solar, Inc., AZ. [Online]. Available: http://www.kyocerasolar.com/pdf/specsheets/.

[8] A. E.-M. M. A. EI-Aal, J. Schmid, J. Bard, and P. Caselitz, "Modeling and optimizing the size of the power conditioning unit for photovoltaic systems," *Journal of Solar Energy Engineering, Transactions of the ASME*, vol. 128, no. 1, Feb. 2006, pp. 40-44.

[9] A. Driesse, P. Jain, and S. Harrison,"Beyond the curves: modeling the electrical efficiency of photovoltaic inverters," in *Proc. 33rd IEEE Photovoltaic Specialists Conference*, 2008, pp.3.

[10] D. King et al., "Performance model for grid-connected photovoltaic inverters," Sandia National Laboratories, Albuquerque, NM, Tech. Rep. SAND2007-5036, Sept. 2007.

[11] H. Neuenstein, "Valiantly defeated – Testing SMAs SB 2100TL inverter," *Photon Magazine*, pp. 144-153, June 2009.

[12] B. Burger and R. Ricardo, "Inverter sizing of grid-connected photovoltaic systems in the light of local solar resource distribution characteristics and temperature," *Solar Energy*, vol. 80, pp. 32- 45, Jan. 2006.

[13] Measurement and Instrumentation Data Center. National Renewable Energy Laboratory, CO. [Online]. Available: http://www.nrel.gov/midc/.

[14] F. P. Baumgartner, H. Schmidt, B. Burger, R. Bruendlinger, H. Haeberlin, and M. Zehner, "Status and relevance of the DC voltage dependency of photovoltaic inverters," in *22nd European Photovoltaic Solar Energy Conference*, Sept. 2007, pp. 2.

[15] C. Harris-Russel. (2010, Mar.). Average retail price of electricity to ultimate customers: Total by end-use sector. U.S. Energy Information Administration: Independent Statistics and Analysis, Washington DC. [Online]. Available: http://www.eia.doe.gov/cneaf/electricity/epm/epm_sum.html.

[16] Database of State Incentives for Renewables & Efficiency: Financial incentives for renewable energy. (2009). N.C. Solar Center, NC. [Online]. Available: http://www.dsireusa.org/summarytables/finre.cfm.

[17] Solar Electricity Prices. (2010, Mar.). Solarbuzz. [Online]. Available: http://www.solarbuzz.com/SolarPrices.htm.